A Generalized Framework for Service Restoration in a Resilient Power Distribution System

Shiva Poudel, *Member, IEEE*, Anamika Dubey, *Member, IEEE*, and Kevin P. Schneider, *Fellow, IEEE*

***Abstract*—An electric power grid is one of the complex infrastructures, and because of its complex nature, there is simply no way that outages can be completely avoided. Thus, a modern society that depends on reliable electric supply requires a resilient electric system that can recover from disruptions while integrating emerging smart grid technologies. This article presents a novel approach for service restoration in a modern power distribution system with controllable switches and distributed generation (DG) resources for any kind of outage. The proposed framework supports both the traditional service restoration using feeder reconfiguration and the grid-forming DG-assisted intentional islands that are dynamically sized using algorithms based on the fault scenario, available resources, and priority of loads. The problem is formulated as a mixed-integer linear program that incorporates critical system connectivity and operating constraints. Simulations are performed to demonstrate the effectiveness of the proposed approach using a large-scale four-feeder 1069-bus three-phase unbalanced distribution test system. It is demonstrated that the framework is effective in utilizing all available resources in quickly restoring the power supply to improve resiliency during extreme events and is scalable for a large-scale unbalanced power distribution system.**

***Index Terms*—Distributed power generation, power distribution, power distribution faults, power system restoration, resilience.**

NOMENCLATURE

$\mathcal{E}^{\mathcal{F}}$	Set of disconnected or opened switches.
$\mathcal{E}_{\mathcal{I}}$	Set of feeder transformers.
$\mathcal{E}_t^{\mathcal{R}}$	Set of normally open tie switches.
$\mathcal{E}_s^{\mathcal{R}}$	Set of normally closed sectionalizing switches.
$\Phi=\{a,b,c\}$	Set of phases of a bus.
$\mathcal{E}$	Set of physical line sections.
$\mathcal{V}$	Set of physical system buses.
$\mathcal{V}^{\mathcal{R}}$	Set of remotely switchable buses.
$\mathcal{E}^{\mathcal{R}}$	Set of switchable lines, i.e., $\mathcal{E}_t^{\mathcal{R}} \cup \mathcal{E}_s^{\mathcal{R}}$.
$\mathcal{E}_c$	Set of switches in a cycle c.
$\mathcal{E}_v$	Set of virtual edges for DG connection.
$\mathcal{T}$	Spanning tree with set of edges.
$P_{i,t}^{\text{grid}}$	Active power demand from grid by i at time t.
v_i	Bus energization variable.
$\lambda_{i,t}^c, \lambda_{i,t}^d$	Charge/discharge status of the ith energy storage (ES) system at time t.
$P_{ij}^{\phi} + \text{j}Q_{ij}^{\phi}$	Complex power flow from i to j for $\phi \in \Phi$.
$P_{i,t}^{E}$	ES active power at bus i at time t.
δ_{ij}	Line or switch decision variable.
s_i	Load pick-up variable.
$\boldsymbol{P}_{ij} + \text{j}\boldsymbol{Q}_{ij}$	Three-phase complex power flow from i to j.
$\boldsymbol{U}_i$	Three-phase voltage magnitude square vector.
$\boldsymbol{V}_i$	Three-phase voltage vector for bus i.
$P_{i,t}^{\text{PV}}$	PV generation at bus i at time t.
$\text{SOC}_{i,t}$	State of charge of battery at bus i at time t.
$\boldsymbol{S}_{ij}^{\text{rated}}$	Apparent power flow limit for $(i,j) \in E$.
η_c, η_d	Charging/discharging efficiency of a battery.
$P_{Li}^{\phi} + \text{j}Q_{Li}^{\phi}$	Complex power demand at i for phase $\phi \in \Phi$.
$P_G^{\max}$	Maximum active power capacity of a DG.
$Q_G^{\max}$	Maximum reactive power capacity of a DG.
$\text{SOC}_{\max}$	Maximum SOC of a battery.
$\text{SOC}_{\min}$	Minimum SOC of a battery.
$\lvert\mathcal{E}_c\rvert$	Number of switches in a cycle c.
$\boldsymbol{S}_{ij}$	Polygon based linearized equivalent of $\boldsymbol{S}_{ij}^{\text{rated}}$.
EC_i	Rated capacity of ES at bus i (in kWh).
$\boldsymbol{r}_{ij}/\boldsymbol{x}_{ij}$	Resistance/reactance matrix of line $i \to j$.
$\boldsymbol{P}_{Li} + \text{j}\boldsymbol{Q}_{Li}$	Three-phase complex load demand at bus i.

Manuscript received June 9, 2020; accepted July 22, 2020. Date of publication August 10, 2020; date of current version March 24, 2022. This work was supported by the U.S. Department of Energy under Contract DE-AC05-76RL01830. *(Corresponding author: Shiva Poudel.)*

Shiva Poudel and Anamika Dubey are with the School of Electrical Engineering, and Computer Science, Washington State University, Pullman, WA 99164 USA (e-mail: shiva.poudel@wsu.edu; anamika.dubey@wsu.edu).

Kevin P. Schneider is with the Seattle Research Center in Seattle, Pacific Northwest National Laboratory, Seattle, WA 98109 USA (e-mail: kevin.schneider@pnnl.gov).

Digital Object Identifier 10.1109/JSYST.2020.3011901

I. INTRODUCTION

INCREASED dependence on an electric power grid coupled with the increasing number of natural disasters motivates the need for improving the resilience of electric power distribution systems [1]. Note that in the aftermath of a natural disaster, 90% of the customers are affected due to damages in power distribution feeders. Improving resilience requires mechanisms to quickly restore the power distribution systems using all available resources. Lately, to enhance distribution system's restoration capability, it is proposed to use distributed generator (DG) resources as community resources by extending their zone of service to other loads and to enable DG-assisted intentional islanding to support grid's critical loads during a major disruption caused by a natural disaster [2], [3].

However, it is nontrivial to incorporate DGs in the distribution system restoration (DSR) problem. First, it is difficult to ensure power flow feasibility in restoration paths when DGs can operate either in islanded or grid-connected modes. Second, multiple possible restoration options provided by DGs, coupled with the numerous sectionalizing switches and tie switches in the distribution grid, significantly increase the complexity of the inherent combinatorial service restoration problem. To address these concerns, in this article, we present a computationally

tractable framework to leverage DGs to restore the service under all disruption scenarios while maintaining the operational feasibility for the restored network.

A. Related Literature

The DSR problem requires feeder reconfiguration and is usually modeled as a combinatorial optimization problem. Earlier research in DSR focused on designing expert systems and heuristic search methods [4], [5] to avoid solving the combinatorial problem. Soft computing algorithms, including genetic algorithm (GA), particle swarm optimization, simulated annealing, and fuzzy set approaches, have also been proposed [6], [7]. Service restoration using mathematical programming for an unbalanced distribution system has been proposed as well by several researchers [8]–[10]. Mathematically, the DSR problem is formulated as a mixed-integer nonlinear program (MINLP). Although accurate, MINLP-based formulations are computationally unattractive as they do not scale well, and the simulation time increases tremendously with the increase in the complexity of the restoration problem.

Another body of work aims at restoring the distribution grid during typical faults or natural disasters with the help of active islanding methods using microgrids and DGs [11]–[14]. For example, restoration algorithms based on spanning tree search have been proposed to restore the critical loads in [11] and [12]. The heuristics employed to search for a restoration plan, however, can be time-consuming. A few proposed methods use DGs to restore loads during an extreme event by partitioning the distribution system into several smaller islanded grids [13], [15], [16]. However, these methods include only a single-phase distribution feeder with no tie switches, making them inapplicable to the actual DSR problem. A few recent articles model the DSR problem for a three-phase system; however, they do not integrate active DG islanding within the DSR problem and show results for a small test case (such as IEEE 34, IEEE 123 bus), thus failing to demonstrate the feeder reconfiguration process during service restoration in a realistic multifeeder test case [17], [18].

B. Literature Gap

Although a vast body of literature exists in the service restoration domain, there remain critical gaps in the literature. First, the methods based on rule-based search or other heuristics, although model a three-phase distribution grid with multiple tie switches and DGs, do not provide mathematical insights, result in suboptimal solutions, and can be time-consuming. Second, methods based on nonlinear programming with mixed-integer constraints, although provide an optimal solution, are computationally intensive and do not scale for a large distribution system with several tie switches and DGs. Third, the existing methods using linear programming, although theoretically scale better than nonlinear methods, do not apply to actual distribution systems with several tie switches and distributed resources and do not model an unbalanced large-scale distribution system. Finally, none of the methods include contributions from nonutility/customer-owned DGs in improving the grid's restoration capability.

C. Specific Contributions

This article aims at bridging the existing gaps in DSR literature by developing a unified service restoration framework that effectively leverages all DG resources, including grid-forming and grid-following technologies, is applicable during both the normal faults and the abnormal disaster scenarios, and is scalable to a large-scale multifeeder three-phase unbalanced distribution grid with multiple DGs/microgrids. Specifically, we model the DSR problem as a mixed-integer linear program (MILP) to maximize the restored loads using all available resources under all fault scenarios while using the least number of switching operations. The specific contributions of this article are listed as follows.

1) *DG-Assisted Restoration During Normal Faults and Disaster Events:* A unified restoration framework is proposed that effectively integrates DG-assisted restoration into the traditional DSR problem. The proposed approach can intentionally island parts of the distribution network to support the critical loads using DGs during extreme conditions. These islands are dynamically sized using the algorithms based on the fault scenario, critical loads, and available resources.

2) *Including Multiple Reconfiguration Possibilities Using Tie Switches, Sectionalizing Switches, and DG Islanding:* The proposed algorithm ensures that the restored network and DG-assisted islands operate in a radial topology by selecting optimal and power flow feasible restoration paths. This combinatorial path search problem is solved by introducing binary decision variables for controllable lines and buses and coupling those to the associated power flow equations.

3) *Integrate Customer-Owned DGs in Grid-Following Mode:* Customer-owned DGs can decrease the generation requirement for DG-assisted island. To include customer-owned DGs into the restoration problem, an optimization model is proposed to obtain probable load demand. Note that customer-owned DGs operate in a grid-following mode within the islands formed by grid-forming DGs. What is grid following

4) *Scalable MILP Formulation for a Three-Phase Unbalanced Multifeeder Distribution Grid:* Several innovations introduced while modeling the MILP problem ensure that the proposed framework easily scales for a large-scale unbalanced three-phase distribution system as the available restoration/reconfiguration options increase due to the addition of a new resource (DG/feeder), new sectionalizing/tie switches, and/or customer-owned DGs.

II. Distribution System Restoration

In this section, the methodology of the proposed approach and graph-theoretic framework is detailed along with a description of decision variables to model the service restoration problem for an unbalanced power distribution system.

A. Methodology

The proposed framework for DSR can be implemented in a modern distribution management system (DMS). Fig. 1 shows the overall architecture of the modern DMS with the

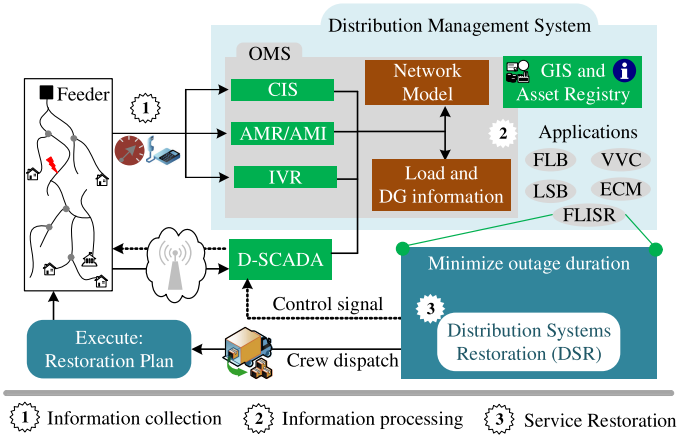

Fig. 1. Architecture of a modern DMS and flowchart of the proposed DSR.

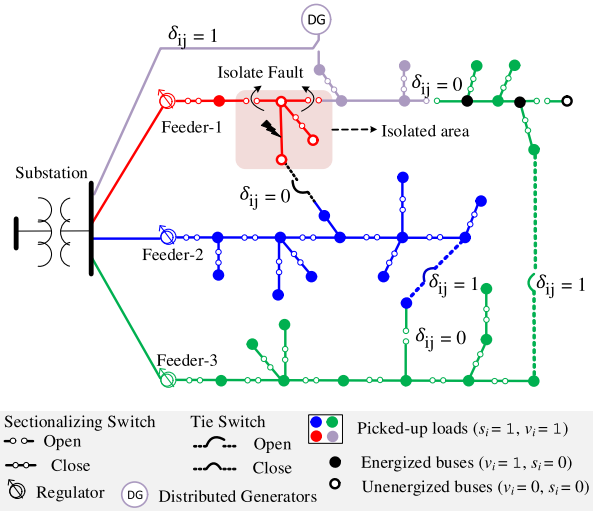

Fig. 2. Example restoration scenario. The colors indicate energized feeder sections and binary variables define the topology of the network.

integration of several subsystems such as customer information system (CIS), geographical information system (GIS), interactive voice response (IVR), advanced metering infrastructure (AMI), supervisory control and data acquisition (SCADA), and flowchart of the proposed DSR framework. Once a power outage is detected, three specific tasks are performed in the DMS to restore the power to the out-of-service area.

Information Collection: After an outage, outage management system (OMS) will collect information via real-time data interface (SCADA) and customer interface (CIS, AMI, and IVR). The information includes statuses of the components and available grid resources to provide distribution system condition monitoring during normal and abnormal conditions.

Information Processing: Once the information is collected, OMS generates an accurate network connectivity model and associated renderings from a GIS system and list of assets (DGs) and their status from an asset registry. Based on the information collected, the fault locations can be pinpointed. The faulty areas can be isolated by opening the switches that are installed along the feeders. Then, the maintenance crews are dispatched to fix the failed components in the isolated faulty areas.

Service Restoration: Once the fault is isolated and the updated system model is identified, the service restoration algorithm is executed to generate an optimal and feasible restoration plan. We describe a mathematical programming approach for service restoration using all available resources, including DERs, in Section III. DSR then energizes the unfaulted portion(s) of the feeder and restores services to the customers using other substations/feeders/DGs (see Fig. 2). Note that if feeders are not available, DGs can be utilized to supply the critical loads.

B. Model Representation

A distribution network is formed by the interconnected distribution feeders and DGs, as shown in Fig. 2. In an efficient restoration plan, several normally open tie switches and normally closed sectionalizing switches are operated to restore the outage loads. Open-loop configurations resulting from the combinations of tie switches and sectionalizing switches will lead to multiple possible radial configurations to restore the loads. The restored distribution system must always operate in a radial configuration, thus requiring a decision upon which switch pairs to operate for restoration. Furthermore, as the time taken by the restoration process depends on the number of switching operations, it is desirable to keep the number of switching operations to a minimum. Note that most of the switches in distribution systems are manually operated that require truck rolls, and it is a time-consuming process.

During an extreme event, DGs can be utilized to increase the amount of load restored by allowing for intentional islanding (see Fig. 2). Note that only utility-owned DGs with grid-forming inverters are employed for intentional islanding. This is important since most DGs do not use expensive grid-forming inverters, and nonutility generation typically cannot wheel power across the utility system. The IEEE Standard 1547-2018 specifies standards for DG-assisted islanding. The possible options for restoration grow significantly when DG-assisted islanding is allowed, requiring a scalable decision-making framework.

We formulate the DSR problem as a multiobjective optimization problem with the joint objective of maximizing the restored loads using a minimum number of switching operations while satisfying the system's operational and connectivity constraints. Intentional islanding using DGs is allowed where the islanded networks satisfy the connectivity and network operating constraints. Note that although customer-owned DGs cannot be used to support or form an active islanded network, they can help offset the generation requirement from grid-forming DGs when operating in the islanded mode. Therefore, we also propose an approach to model contributions from customer-owned DGs in the restoration problem. The problem definition and constraints are detailed in Section III.

C. Graphical Representation of the Distribution Network

We represent the associated distribution network comprised of multiple feeders and DGs using a connected graph, $G(V, E)$, where buses are modeled as vertices and physical line sections, including switches as edges. The DSR problem identifies a

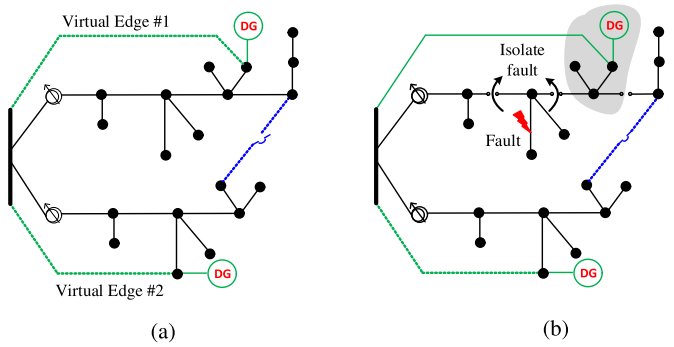

Fig. 3. Operating modes of grid-forming DGs. (a) DG connected to main network (normal operation). (b) Formation of DG island (restoration mode).

desired subtree within the graph, G, that maximizes a given objective function subject to various connectivity and operating constraints. The binary variables associated with the problem are defined as follows.

1) Bus Energization Variable: A binary variable $v_i = \{0, 1\}$ is assigned to each bus, where $v_i = 1$ implies that bus i is energized, while $v_i = 0$ implies that bus i is not energized during the restoration process.

2) Load Pick-Up Variable: Each load bus is assigned a binary variable $s_i = \{0, 1\}$ that represents the switch status of the load connected to a particular bus. This variable helps in the case when only a few critical loads are to be restored without restoring all the loads in the path. Note that for a load to be restored, both s_i and v_i must be 1.

3) Line/Switch Variable: A binary variable $\delta_{ij} = \{0, 1\}$ is associated with each line sections including switches, where $\delta_{ij} = 1$ implies that switch joining buses i and j is closed, while $\delta_{ij} = 0$ implies switch is open. The decision on the line/switch binary variable helps maintain a radial configuration for the restored network. The line variable will be used to formulate power flow constraints and connectivity constraints for the associated distribution network.

4) Grid-Forming DG Status Variable: The complexity of the restoration problem in the distribution system increases significantly in the presence of grid-forming DGs when intentional islanding is allowed. To formulate a unified DSR problem that enables restoration using both DG islands and other feeders, a virtual edge, δ_{ij}, is added between the subtransmission bus and each grid-forming DG, as shown in Fig. 3(a). The state of this edge determines whether the DG is connected to the main network or an island is formed. If the virtual edge is closed, i.e., $\delta_{ij} = 1$, DG located at bus j operates in the islanded mode. Note that this DG is virtually connected to subtransmission bus i [see Fig. 3(a)] and, therefore, is able to inject three-phase apparent power $\boldsymbol{P}_G + \mathrm{j}\boldsymbol{Q}_G$ to bus j. However, to avoid the possible loop configuration, one of the switches in the distribution network is opened by the DSR algorithm. This ensures an islanded operation of DG, as shown in Fig. 3(b).

III. Problem Formulation

In this section, we detail the mathematical formulation for the restoration problem described in Section II.

A. Problem Objective

The problem objective is to maximize the restored load and minimize the switching operations subject to feeder's operational and connectivity constraints.

1) Maximize the Restored Load: The first objective is to maximize the amount of load restored while considering different weight factors for each load (w_i) that indicate load priority. The objective is defined as follows:

$$\text{Max.} \sum_{i\in\mathcal{V}} \sum_{\phi\in\{a,b,c\}} w_i \; s_i \; P_{Li}^{\phi}. \tag{1}$$

2) Minimize the Number of Switching Operations: The number of switching operation determines the performance of the restoration plan as it closely relates to the time taken to execute the restoration plan. In addition, frequently operating switches adds additional maintenance cost. Therefore, it is desirable to minimize the number of switching operations so that the restoration plan can be executed in an efficient and timely manner. Thus, the second objective is to minimize the total number of switching operations defined as

$$\text{Min.} \left(\sum_{(i\to j)\in\mathcal{E}_s^{\mathcal{R}}} (1-\delta_{ij}) + \sum_{(i\to j)\in\mathcal{E}_t^{\mathcal{R}}} \delta_{ij} + \sum_{(i\to j)\in\mathcal{E}_v} \delta_{ij} \right). \tag{2}$$

3) Weighted Objective Function: We define a multiobjective restoration problem using a weighted combination of the two previously defined objective functions

$$\text{Min.} \left(-\alpha \sum_{i\in\mathcal{V}} \sum_{\phi\in\{a,b,c\}} w_i \; s_i \; P_{Li}^{\phi} + \beta \left(\sum_{(i\to j)\in\mathcal{E}_s^{\mathcal{R}}} (1-\delta_{ij}) + \sum_{(i\to j)\in\mathcal{E}_t^{\mathcal{R}}} \delta_{ij} \right) + \gamma \sum_{(i\to j)\in\mathcal{E}_v} \delta_{ij} \right). \tag{3}$$

As the customer's satisfaction depends upon the availability of the power supply, the maximization of the restored load is defined as the primary objective and is always given a higher preference. The weights α, β, and γ are defined such that the primary objective is always prioritized. Since the secondary objective is a sum of binary variables only, making $\beta < 1, \gamma < 1$, and assigning α a large number ensures that the problem first restores the maximum weighted loads and then minimizes the switching operations. In addition, DGs must not operate in an islanded mode unless it is required. Thus, the priority for restoration is to use feeder backup by switching a pair of sectionalizing and tie switches. When a normally open tie switch operates, a normally closed sectionalizing switch has to be opened to maintain a radial topology. Thus, gamma is made at least $2|\mathcal{E}_t^{\mathcal{R}}|$ times higher than β (i.e., $\gamma \geq 2|\mathcal{E}_t^{\mathcal{R}}|\beta$).

B. Problem Constraints

Several constraints associated with the proposed service restoration problem are described in this section.

1) Connectivity Constraints: This section defines the set of topological constraints required to ensure a connected network for the restored loads and a radial restored network topology.

1) Constraint (4a) ascertains that a load with a switch can be picked up if and only if it is connected to a bus that is

energized in the restored network by one of the feeders or DGs. Constraint (4b) ensures that a nonswitchable load will be energized depending upon the associated bus energization variable. Thus, a nonswitchable load is always picked up if the corresponding bus is energized.

$$s_i \leq v_i \;\; \forall i \in \mathcal{V}^{\mathcal{R}} \tag{4a}$$

$$s_i = v_i \;\; \forall i \in \mathcal{V} \backslash \mathcal{V}^{\mathcal{R}} \tag{4b}$$

2) The constraints for decision upon line energization variable, (δ_{ij}), are defined in (5a)–(5d). The set of equations implies that the decision on lines to be used in the restoration depends upon the corresponding buses and their energization statuses. Equation (5a) ensures that if a line with a switch is energized, the buses connecting the line must be energized. Equation (5b) ensures that a line without switch must be energized if any of the buses connecting it is energized. The faults and the open switches in the distribution network are modeled using (5c). For a disaster case, a substation fault is included using (5d), which implies all the feeders are disconnected from the main supply

$$\delta_{ij} \leq v_i, \; \delta_{ij} \leq v_j \; \forall (i \to j) \in \mathcal{E}^{\mathcal{R}} \backslash \mathcal{E}^{\mathcal{F}} \tag{5a}$$

$$\delta_{ij} = v_i = v_j \;\; \forall (i \to j) \in \mathcal{E} \backslash (\mathcal{E}^{\mathcal{R}} \cup \mathcal{E}^{\mathcal{F}}) \tag{5b}$$

$$\delta_{ij} = 0 \;\; \forall (i \to j) \in \mathcal{E}^{\mathcal{F}} \tag{5c}$$

$$\delta_{ij} = 0 \;\; \forall (i \to j) \in \mathcal{E}_{\mathcal{I}} \tag{5d}$$

3) A new radial configuration of the faulted distribution system is achieved by closing and opening the appropriate tie switches, sectionalizing switches, and virtual edges. A radial topology for restored networks is ensured using (6) that enforces at least one of the switches in any cycle to be open. All possible cycles in a distribution network are enumerated using an iterative loop counting algorithm, which is a "brute force" technique [19]. Then, (6) is written for each cycle. The number of cycles in a graph increases with the increase in the number of tie switches. Despite that, G is usually sparse for a distribution network, where the total number of cycles is much less than $2^{|\mathcal{V}|}$. It is important to note that this enumeration can be done offline by storing all the cycles as it is fixed for a given in-build distribution network. Thus, the enumeration approach does not affect the real-time computational complexity.

$$\sum_{(i \to j) \in \mathcal{E}^c} \delta_{ij} \leq |\mathcal{E}^c| - 1 \qquad \forall (i \to j) \in \mathcal{E}^c \tag{6}$$

2) Power Flow Constraints: A three-phase linearized ac power flow model for the unbalanced distribution system proposed in [20] is used in this article. The linearized model is sufficiently accurate and applicable for restoration problems [20]. The linearized model for the 1096-bus test system incurs the largest errors of 2.56% and 0.002 p.u. in apparent power flow and bus voltages, respectively, compared to the actual power flow solution obtained using OpenDSS. The restoration problem requires the decision upon which lines are energized while accounting for network operating constraints. The power flow along a line is only valid if the line is energized. Therefore, to appropriately represent the restoration problem, the branch flow equations are coupled with line and bus decision variables.

1) Constraints (7a)–(7c) represent three-phase unbalanced linearized power flow equations coupled with line decision variable δ_{ij} and load pick-up variable s_i. Note that $\delta_{ij} = 1$, if $(i \to j) \in \mathcal{E} \backslash (\mathcal{E}^{\mathcal{R}} \cup \mathcal{E}^{\mathcal{F}})$. Constraint (7a) defines voltage equations where if two buses i and j are connected without a remotely switchable line or if the line is energized, the voltage difference of the branch is then constrained by the branch power flow. Similarly, (7b) and (7c) define active and reactive power flow constraints that must be satisfied for each energized line. Note that (7a)–(7c) are nonconvex as they involve product of variables. These constraints are linearized by defining an auxiliary variable and using big-M method [21].

$$\delta_{ij} \left(\boldsymbol{U}_i - \boldsymbol{U}_j \right) = 2 \left(\tilde{\mathbf{r}}_{ij} \boldsymbol{P}_{ij} + \tilde{\mathbf{x}}_{ij} \boldsymbol{Q}_{ij} \right) \qquad \forall (i,j) \in \mathcal{V} \tag{7a}$$

$$\sum_{(i \to j) \in \mathcal{E}} \delta_{ij} \boldsymbol{P}_{ij} = s_j \, \boldsymbol{P}_{Lj} + \sum_{\substack{(j \to c) \in \mathcal{E} \\ i \neq c}} \delta_{jc} \boldsymbol{P}_{jc} \;\; \forall (i,j) \in \mathcal{V} \tag{7b}$$

$$\sum_{(i \to j) \in \mathcal{E}} \delta_{ij} \boldsymbol{Q}_{ij} = s_j \, \boldsymbol{Q}_{Lj} + \sum_{\substack{(j \to c) \in \mathcal{E} \\ i \neq c}} \delta_{jc} \boldsymbol{Q}_{jc} \;\; \forall (i,j) \in \mathcal{V} \tag{7c}$$

where $\tilde{\mathbf{r}}_{ij} = \text{Real}\{\alpha\alpha^H\} \otimes \mathbf{r}_{ij} + \text{Im}\{\alpha\alpha^H\} \otimes \mathbf{x}_{ij}, \tilde{\mathbf{x}}_{ij} = \text{Real}\{\alpha\alpha^H\} \otimes \mathbf{x}_{ij} + \text{Im}\{\alpha\alpha^H\} \otimes \mathbf{r}_{ij}$, and $\alpha = [1 \; e^{-j2\pi/3} \; e^{j2\pi/3}]^T$

3) Voltage Regulator and Capacitor Banks Models: For a large feeder, voltage regulators (VRs) and capacitor banks (CBs) may help restore additional loads that might not be possible due to potential undervoltage issues. In this section, we derive a mathematical model for VRs and CBs, where VR tap position and CB status are modeled as binary variables.

A 32-step VR with a voltage regulation range of $\pm 10\%$ is assumed. Let a_ϕ be the turn ratio for the VR connected to phase ϕ of line (i,j). Then, a_ϕ can take values between 0.9 and 1.1 with each step resulting in a change of 0.00625 p.u. Let $u^{\phi}_{\text{tap},i} \in \{0,1\}$ be a binary variable defined for each regulator step position, i.e., $i \in (1,2,\ldots,32)$. Define a vector $b_i \in \{0.9, 0.90625, \ldots, 1.1\}$. Then, $V_j^{\phi} = a_\phi V_i^{\phi}$, where $a_\phi = \sum_{i=1}^{32} b_i u^{\phi}_{\text{tap},i}$ and $\sum_{i=1}^{32} u^{\phi}_{\text{tap},i} = 1$. Taking square of voltage equation, defining $a_\phi^2 = A_\phi$, $b_i^2 = B_i$, and realizing that $(u^{\phi}_{\text{tap},i})^2 = u^{\phi}_{\text{tap},i}$, we obtain (8), representing model for the VR. Note that if a multiphase VR is gang operated, a single A^ϕ and $u^{\phi}_{\text{tap},i}$ variables are defined for each phase.

$$\boldsymbol{U}_j = A^{\phi} \boldsymbol{U}_i \tag{8}$$

The reactive power generated by CB, $q^{\phi}_{\text{cap},i}$, is defined as a function of binary control variable $u^{\phi}_{\text{cap},i} \in \{0,1\}$ indicating the status (ON/OFF) of the CB, its rated per-phase reactive power $q^{\text{rated},\phi}_{\text{cap},i}$, and the square of the bus voltage at bus i for phase ϕ, U_i^{ϕ}, in (9). The CB model is assumed to be voltage dependent and provides reactive power as a function of U_i^{ϕ} when connected, i.e., $u_{\text{cap},i} = 1$. For a three-phase CB, a common control variable $u^{\phi}_{\text{cap},i}$ is defined for each phase as

$$q^{\phi}_{\text{cap},i} = u^{\phi}_{\text{cap},i} q^{\text{rated},\phi}_{\text{cap},i} U_i^{\phi}. \tag{9}$$

Both (8) and (9) include a product of binary and continuous variables that can be easily linearized using the big-M method.

4) Network Operating Constraints: This section defines nodal voltage limit constraints and thermal limit constraints for lines and transformers.

1) The voltage of each bus should be within the limit as specified in ANSI C84.1 and is ensured by (10). $\boldsymbol{U}^{\min}$ and $\boldsymbol{U}^{\max}$ are set to $(0.95)^2$ and $(1.05)^2$, respectively, for each phase of the bus.

$$v_i \boldsymbol{U}^{\min} \leq \boldsymbol{U}_i \leq v_i \boldsymbol{U}^{\max} \;\; \forall i \in \mathcal{V} \tag{10}$$

2) The loading on the lines and transformers must not exceed the rated kVA capacity. The rated kVA capacity is specified for the transformers. The thermal limit for the lines is, however, specified in terms of their ampacity. We use a nominal feeder voltage of 1 p.u. to convert line ampacity rating to their rated kVA capacity. The actual thermal limit constraint is specified using the quadratic equation in (11). We use the polygon-based linearization approach proposed in [22] to linearize (11) by a set of linear constraints defined in (12). We use (12) instead of (11) in the MILP model.

$$(\boldsymbol{P}_{ij})^2 + (\boldsymbol{Q}_{ij})^2 \leq \left(\boldsymbol{S}_{ij}^{\text{rated}}\right)^2 \;\; \forall (i \to j) \in \mathcal{E} \tag{11}$$

$$\begin{aligned} -\sqrt{3}\,(\boldsymbol{P}_{ij} + \boldsymbol{S}_{ij}) \leq \boldsymbol{Q}_{ij} \leq -\sqrt{3}\,(\boldsymbol{P}_{ij} - \boldsymbol{S}_{ij}) \\ -\sqrt{3}/2\;\boldsymbol{S}_{ij} \leq \boldsymbol{Q}_{ij} \leq \sqrt{3}/2\;\boldsymbol{S}_{ij} \\ \sqrt{3}\,(\boldsymbol{P}_{ij} - \boldsymbol{S}_{ij}) \leq \boldsymbol{Q}_{ij} \leq \sqrt{3}\,(\boldsymbol{P}_{ij} + \boldsymbol{S}_{ij}) \end{aligned} \tag{12}$$

where $\boldsymbol{S}_{ij} = \boldsymbol{S}_{ij}^{\text{rated}} \sqrt{(2\pi/n)/\sin(2\pi/n)}$ and $n = 6$.

5) DG Operating Constraints: Constraint (13) ensures that the in-flow power of each DG from the subtransmission bus should be less than or equal to the rated DG capacity. This is per the fact that all DGs are connected to subtransmission bus using virtual edges.

$$\sum_{\phi \in \{a,b,c\}} P_{ij}^{\phi} \leq \delta_{ij} P_G^{\max}\,, \quad \sum_{\phi \in \{a,b,c\}} Q_{ij}^{\phi} \leq \delta_{ij} Q_G^{\max} \tag{13}$$

C. Integrating Customer-Owned Grid-Following DGs

Owing to push toward a sustainable energy future, it is anticipated that the penetrations of customer-owned DGs (rooftop photovoltaics (PVs) and energy storage (ES) systems) will increase. It is also anticipated that for improved efficiency, customers will take greater control of their electricity usage by optimally managing their DGs [23]. Although customer-owned DGs cannot be used to form intentional islands, they can help offset generation requirements from utility-owned DGs during intentional islanding by reducing the aggregated load demand for the customer. This makes it desirable to include generation from customer-owned DGs into the restoration problem.

In this section, we present a method to obtain a representative load demand for distribution customers with customer-owned DGs. The probable load demand for each customer is obtained assuming that the customer-owned DGs are optimally scheduled using a home management system (HMS). The obtained load demand is used as input to the restoration problem defined in (1)–(13). Customer-owned DGs always operate in the grid-following mode.

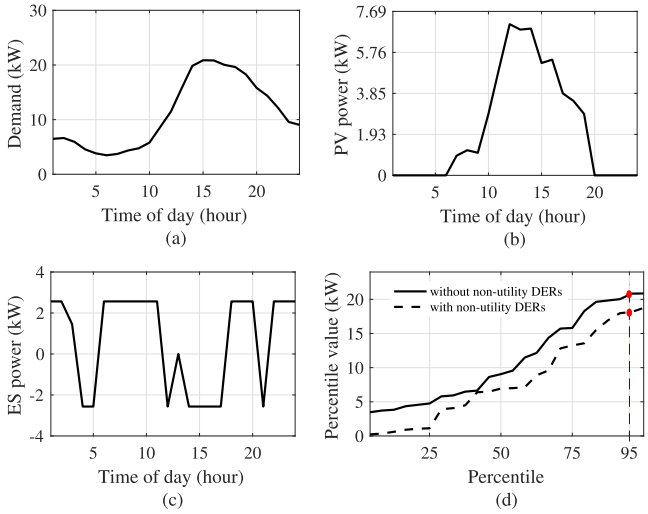

Fig. 4. Customer-owned DGs. (a) Load profile. (b) PV profile. (c) Schedule of the ES device. (d) Percentile plot for aggregated load.

The method to obtain probable load demand for a house with PV and ES is detailed here. First, for each load bus (home) with customer-owned DGs, the forecasted values of load consumption and PV generation are used to obtain an optimal schedule for ES using a linear programming model defined in (14). After solving the optimization problem, the daily profile for forecasted load, PV, and optimal ES schedule is summed up to obtain an aggregated load demand profile for the day. A percentile plot is generated for the aggregated load profile that is used to obtain a single representative value of the customer load to be used in the restoration problem. Allowing a small risk, we choose a 95th percentile load demand as the input to the restoration problem (see Fig. 4). For a customer with only PV, we simply sum up the forecasted load demand and PV generation to obtain the aggregated load and its 95th percentile value. Additional complexity can be embedded in the formulation depending upon DGs and HMS.

$$\text{Minimize:} \sum_{t}^{t+T_H} CP_{i,t}^{\text{grid}} \tag{14}$$

$$\boldsymbol{P}_{i,t}^{\text{grid}} = \boldsymbol{P}_{Li,t} - \boldsymbol{P}_{i,t}^{E} - \boldsymbol{P}_{i,t}^{\text{PV}}$$

$$-\lambda_{i,t}^{c}\,\boldsymbol{P}_{i,t}^{ch,\max} \leq \boldsymbol{P}_{i,t}^{E} \leq \lambda_{i,t}^{d}\,\boldsymbol{P}_{i,t}^{dch,\max}$$

$$\text{SOC}_{i,t} = \text{SOC}_{i,t-1} - \frac{T}{EC_i}\left(\lambda_{i,t}^{d}\,\boldsymbol{P}_{i,t}^{E}\,\eta_d^{-1} + \lambda_{i,t}^{c}\,\boldsymbol{P}_{i,t}^{E}\,\eta_c\right)$$

$$\text{SOC}_i^{\min} \leq \text{SOC}_{i,t} \leq \text{SOC}_i^{\max} \text{ and } \lambda_{i,t}^{c} + \lambda_{i,t}^{d} \leq 1.$$

D. Modeling Outage

A component-level fragility curve is used to model the impacts of extreme events such as hurricanes or other high-speed wind events on power systems [24]. A fragility function maps the probability of failure of distribution system components

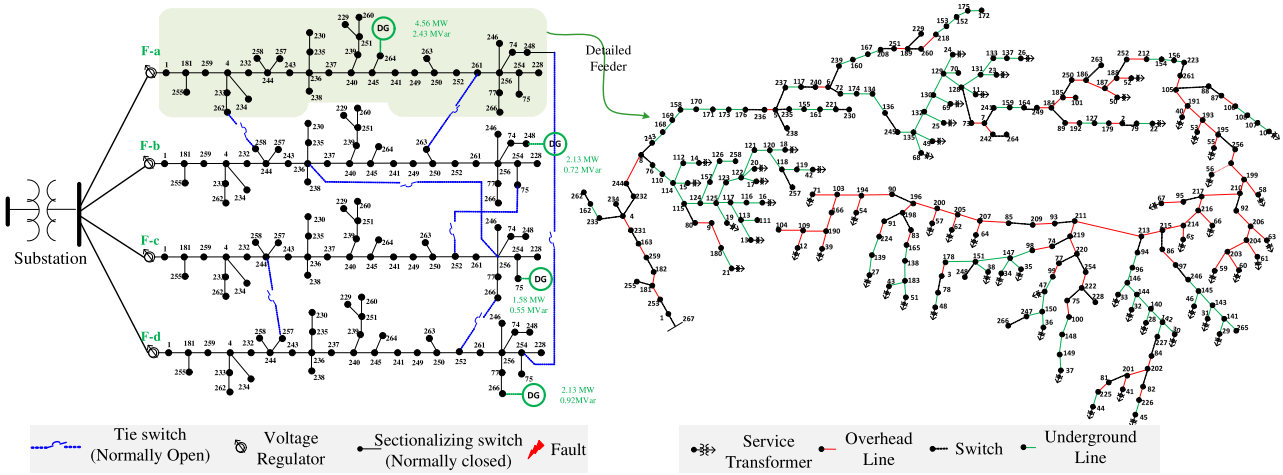

Fig. 5. Simplified one-line diagram of the multifeeder 1069-bus distribution system with seven additional tie switches and four DGs.

conditioned on the intensity of the hazard (e.g., a wind speed). As an example, the failure probability function as a function of wind speed is defined as follows:

$$P_l(\omega) = \begin{cases} P_l^n, & \text{if } \omega < \omega_{\text{critical}} \\ P_l(\omega), & \text{if } \omega_{\text{critical}} < \omega < \omega_{\text{collapse}} \\ 1, & \text{if } \omega > \omega_{\text{collapse}} \end{cases}$$

where $P_l(\omega)$ is the failure probability of a component as a function of wind speed, ω; P_l^n is the failure rate at normal weather condition; and ω_{critical} is the wind speed at which the failure probability rapidly increases. The equipment has a negligible probability of survival at ω_{collapse}.

To model an extreme event, we use the fragility curve to obtain the probability of damage for the given wind speed (associated with the extreme event). The outages are generated by associating a binary variable with the status of the line/buses. The number of such outages depends upon the probability of damage for a given wind speed [25].

IV. Results and Discussions

The effectiveness of the proposed approach is validated using a multifeeder 1096-bus test system consisting of four R3-12.47-2 PNNL taxonomy feeders connected using several tie switches [26]. The restoration problem is formulated as an MILP that can be solved using off-the-shelf solvers. We have used MATLAB R2016a to build the MILP model that is linked to the CPLEX 12.6 solver. The simulation is carried out on a PC with 3.4-GHz CPU and 16-GB RAM.

The taxonomy feeder R3-12.47-2 is a representation of a moderately populated urban area. The total load on the feeder is 4366.955 kW and 1299.206 kVAr. Four identical feeders are replicated to obtain the four-feeder 1069-bus distribution system, where feeders are interconnected using seven normally open tie switches (see Fig. 5). With a total of 1069 multiphase physical buses (3444 single-phase buses), 152 sectionalizing switches, 190 possible cycles, and 122 and 586 normal operational radial topologies, the 1069-bus test case is a sufficiently large-scale model. We also incorporate several grid-forming utility-owned DGs and grid-following customer-owned DGs in test cases. The capacity of utility-owned DGs is shown in Fig. 5. To ensure the ability to transfer the load to other feeders, the feeder loading is limited to 70%; consequently, the feeder transformer capacity is 6.7 MVA.

A. Restoration During Typical Outages

This section simulates typical outage scenarios for the test system with a few lines at fault. It is assumed that the main supply, i.e., the connection to the subtransmission bus, is intact. For minor outages, we assume equal weights for all system loads. Several fault scenarios are simulated to demonstrate the effectiveness of the proposed approach, as shown in Table I. Two different case studies are done for each event: *Case I:* switching scheme without DGs and *Case II:* switching scheme with DGs. Note that notations **F**, **T**, and **I** denote faulted line, tripped switch, and isolation candidate, respectively, for a particular event.

Scenario 1 simulates a fault near feeder F-c (line 253-181). As a result, an upstream switch 267-1 is tripped. Once the faulted zone is identified or the faulty network element is located (a problem we assume solved), an additional switch in F-c is opened (259-183) for isolating the fault to ensure that the faulted zone is not fed during the circuit reconfiguration. It is observed that 4366.95 kW of the load remains unserved. The switching scheme generated from the optimization is to open three sectionalizing switches and close four tie switches. With this restoration plan, 3904.56 kW of the load is restored. Next, the same scenario is simulated for the case that allows intentional islanding using grid-forming DGs. Unlike the previous case, the switching scheme restores 4197.55 kW of the outage loads and requires a total of 11 switching operations, including the formation of two DG-supplied islands (see Table I). The DGs located at F-b and F-c pick up loads and form separate islands to free the feeder-head transformer capacity to help restore additional loads.

Scenario 2 simulates a mid-feeder fault at F-b. Switch 185-250 trips off because of the fault, and two more sectionalizing switches 188-252 and 186-263 are opened for fault isolation.

TABLE I
RESTORATION STRATEGY FOR THE FOUR-FEEDER 1069-BUS TEST CASE WITH AND WITHOUT DGS

Event Detail	**Case 1**: Switching Schemes without DGs		**Case 2**: Switching Schemes with DGs		Load Restored (kW)	
	Open	Close	Open	Close	**Case 1**	**Case 2**
F: 253-181 (F-c) **T**: 267-1 (F-c) **I**: 259-182 (F-c) **Loss**: 4366.95 kW	219-74 (F-a) 222-75 (F-b) 185-250 (F-b)	248-254 (F-a and F-d) 75-252 (F-b and F-c) 236-256 (F-b and F-c) 261-263 (F-a and F-b)	219-74 (F-b) 220-77 (F-c) 220-254 (F-c) 223-261 (F-c) 220-254 (F-d)	DG-248 (F-b) DG-75 (F-c) 248-254 (F-a and F-d) 236-256 (F-b and F-c) 266-252 (F-c and F-d) 244-257 (F-c and F-c)	3904.56	4197.55
F: 187-50 (F-b) **T**: 185-250 (F-b) **I**: 188-252 (F-b) & 186-263 (F-b) **Loss**: 3564.73 kW	195-256 (F-c)	236-256 (F-b and F-c) 75-252 (F-b and F-c)	195-256 (F-c)	236-256 (F-b and F-c) 75-252 (F-b and F-c)	3548.32	3548.32
F: 135-132 (F-d) **T**: 136-245 (F-d) **I**: 128-73 (F-d) **Loss**: 4102.80 kW	220-254 (F-d) 5-237 (F-b) 195-256 (F-c)	248-254 (F-a and F-d) 266-252 (F-c and F-d) 75-252 (F-b and F-c) 236-256 (F-b and F-c)	220-254 (F-d) 220-254 (F-c) 195-256 (F-c)	248-254 (F-a and F-d) 266-252 (F-c and F-d) DG-75 (F-c) DG-266 (F-d)	2984.16	3465.16

Note that the second sectionalizing switch is opened to make sure that the faulted zone is not fed from F-a with the help of a tie switch (261-263 F-a and F-b). The loss of load for this event is 3564.3 kW, including load at node 22, which is in the faulted zone. The restoration solution for this scenario is to open one sectionalizing switch and close two sectionalizing switches, as shown in Table I. Except for load at node 22, all the outage loads are picked up, and also, it is observed that there is no need for any DG support in restoration. Thus, the solution for Cases I and II remains the same.

Scenario 3 simulates a fault at F-d. The corresponding switches that tripped off for protection and fault isolation are shown in Table I. There is an outage section with 4102.80 kW of loads. There is a load transfer scenario between F-b and F-c while restoring the loads with help of tie switches and the restoration plan can pick 2984.16 kW of loads. Besides, with the help of DGs in F-c and F-d, additional loads are picked up with island formation.

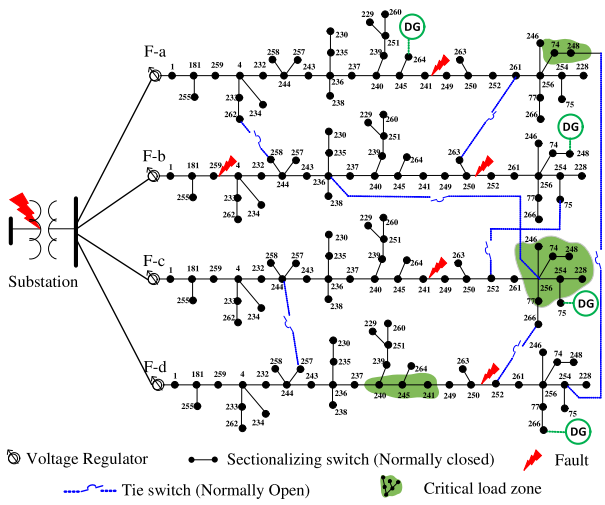

Fig. 6. Test distribution system after a major disaster. The substation is at fault, and multiple distribution system components are damaged.

B. Restoration During an Extreme Event

This section demonstrates the applicability of the proposed approach for restoration during extreme events and validates its effectiveness in handling the disaster conditions. Several case studies demonstrate the applicability of the proposed framework in improving resilience to extreme events using grid-forming DGs, tie switches, and customer-owned DGs.

1) DG Islanding and Impact of Tie Switches in Improving Restorability: It is assumed that the test system has experienced an extreme event resulting in a fault at the substation disconnecting all feeders from the main grid. Besides, several distribution lines are at fault due to damage in the distribution network. The specific disaster scenario is shown in Fig. 6. Due to the scarcity of DG power capacity and lack of enough local generation resources, the critical loads are prioritized over noncritical loads. The critical load zones are represented by green patches in Fig. 6. It is demonstrated that using the proposed approach, the available DGs successfully form self-sustained islands by picking up the critical loads. On average, it takes 12.23 s to obtain a feasible restoration plan.

Two case studies are simulated: *Case I:* with no tie switches and *Case II:* with all seven tie switches available for restoration. Fig. 7 shows the result of a resilient restoration solution for both cases. For Case I, each DG can only pick up the critical loads within their feeders as there are no tie switches available. The total weighted load restored in the distribution network is 6734.265 kW. It is observed that the critical loads in F-a and F-d are not restored because they cannot be reached by their respective DGs due to faults within the distribution system (see Fig. 6). Similarly, the critical load in F-c is partially restored due to the limited capacity of DG-075 in F-c. It is also observed that DG-264 in F-a has excess unused capacity. The unavailability of the paths from DGs to critical loads makes it impossible to supply all critical loads. Case II incorporates all seven tie switches in the restoration process. Unlike the previous case, DGs can expand their electrical boundaries with the help of tie switches forming larger islanded networks (see Fig. 7). With the help of tie switches, the total amount of restored load increases to 9130.11 kW. Thus, tie switches help better restore critical services by providing added operational flexibility.

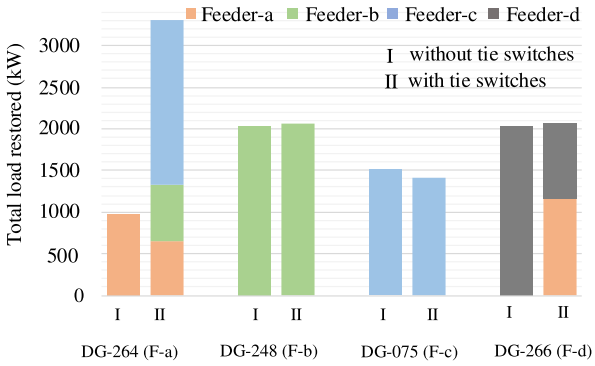

Fig. 7. Total load picked up by each DG in different feeders for a given disaster scenario in Fig. 6. In Case II, DG at a particular feeder restores loads in another feeder by increasing its operational boundary using tie switches.

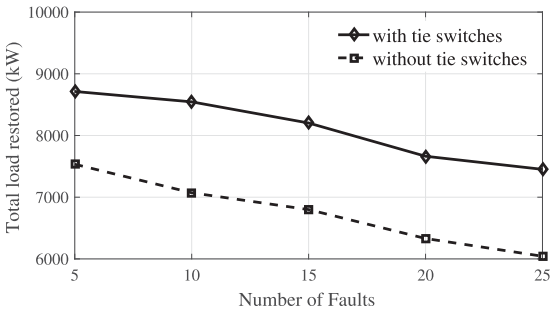

Fig. 8. Impact of damages on restoration plan (random faults simulated with and without considering tie switches).

Next, several random faults within the distribution network are simulated in addition to the substation fault, and their effect on the restoration plan is studied. Note that the fault location shown in Fig. 6 is not valid for this specific case, and we create a random damage scenario for studying the impacts of damage. However, the DG locations and parameters are the same as identified in Section IV-A. As the damage scenario in a distribution network during an extreme event is unpredictable, several scenarios are created to mimic varying damage severity during the disaster condition. Specifically, five different scenarios are simulated, where the number of random faults in the distribution system is 5, 10, 15, 20, and 25, respectively. Fig. 8 shows the total load restored (kW) for each of the randomly generated faults. It is observed that the ability of DGs to provide service is degraded with the increase in physical damage in the distribution network. This is because feasible paths to reach high priority loads decrease, thus decreasing the restoration performance. In contrast, for a given damage scenario, well-placed tie switches improve the restoration ability by providing alternate restoration paths (see Fig. 8). The results validate that the restoration performance is improved in postdisaster condition using active islanding methods and with the help of tie switches.

2) Impacts of DG Dispersion on Restorability: In this case, we study the impact of DG dispersion in improving the resilience of the distribution system. In addition to four utility-owned DGs (with grid-forming technology), four additional utility-owned DGs are installed. The total installed capacity of DGs is made equal for both cases: with four DGs versus eight DGs. The new DGs are located at buses: DG-248 (F-a), DG-264 (F-b), DG-264 (F-c), and DG-264 (F-d). To study the effect of DG dispersion, several random faults within the distribution network are simulated in addition to the substation fault, and their effect on the restoration plan is studied. Specifically, five different scenarios are simulated where the number of random faults in the distribution system is 5, 10, 15, 20, and 25, respectively. To capture the stochastic fault locations, a total of 50 runs are simulated for each fault scenario by varying the locations of faulted lines within the distribution feeder.

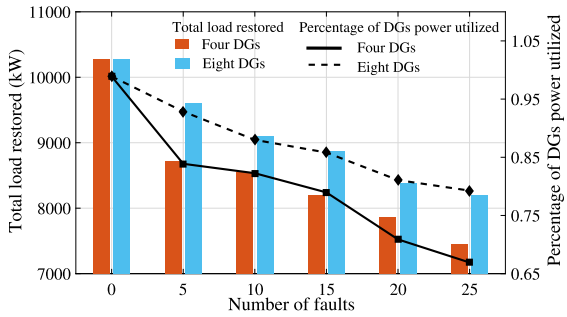

Fig. 9. Impacts of DG dispersion in the distribution network.

Fig. 9 shows the total load restored in kilowatt for the system with four DGs versus eight DGs for each of the randomly generated faults. It is observed that regardless of the extent of damage in the distribution system, the restored load is higher with eight DGs compared to the case with four DGs even though the total installed DG capacity is the same for both cases. This is because, with the increase in the number of faults, DGs have to limit their operational boundary resulting in underutilization of their capacity. Thus, several smaller grid-forming DGs dispersed in the distribution network provide better restoration ability during an extreme event compared to fewer large DGs.

3) Impacts of Customer-Owned DGs in Improving Restorability: In this case, we study the effect of customer-owned DGs in enhancing the restoration capability of a damaged distribution network. A case study with 50 scenarios of 25 randomly generated faults is simulated. It is observed that, on average, the total load restored without including customer-owned DGs is 7486.1 kW. Next, a few loads are installed with DGs. The size of DGs (PV + ES) installed at a load bus is approximately half the size of its peak load demand. Refer to [27] and [28] for optimal sizing and placement. The customer penetration level or the number of loads with customer-owned DGs is varied from 0% to 50%. The test system includes a total of 248 load buses. The number of load buses with customer-owned DGs is calculated based on the penetration level, while their locations are randomly selected. Using the method detailed in Section III-C, the 95th percentile value of aggregated load demand is obtained. Table II summarizes the parameters for loads with customer DGs.

Fig. 10 shows the impacts of incorporating contributions from small-scale customer-owned DGs in enhancing the restoration capability during an extreme event. The DGs decrease the required customer load demand, thus allowing the limited capacity grid-forming DG technology to restore additional system loads. For example, in the case of 20% customer penetration, the additional load restored is about 234.6 kW, and it increases to 457.1 kW for 50% customer penetration level.

TABLE II
CUSTOMER-OWNED DG PENETRATION PARAMETERS (AVERAGE OF 50 SCENARIOS WITH RANDOM DG LOCATIONS)

Penetration level	0%	10%	20%	50%
Total no. of buses with DG	0	24	48	124
Total peak load of buses with DG	–	1442.7	2860.0	7077.8
Total DG capacity (PV+batt.)	–	721.35	1430.25	3538.9
Average 95^{th} percentile load	–	1269.6	2516.8	6228.5

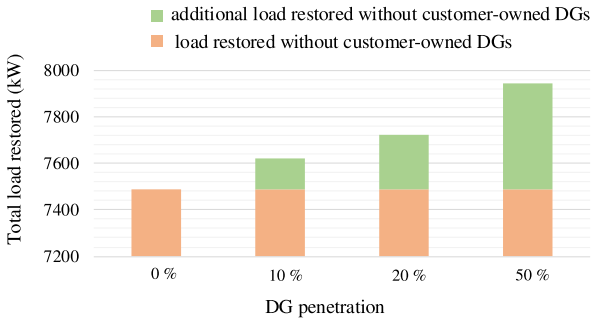

Fig. 10. Impact of customer-owned DGs in improving restoration capability during an extreme event (substation fault and 25 faults in distribution grid).

V. DISCUSSIONS

A. Economic Analysis

In this subsection, we highlight the need for enhancing the resilience of the power grid through the deployment of smart grid technologies, tools, and practices. We also discuss the investment made from the electric power industry, federal and local governments, and socioeconomic benefits of such smart grid technologies to enhance the reliability and resilience of the nation's power grid.

Having the ability to restore the power as quickly as possible following the extreme events, such as Superstorm Sandy and Hurricane Irene, provides economic and public health and safety benefits for local businesses and communities [29]. Based on the power outage data collected by the U.S. Department of Energy's (DOE) Office of Electricity Delivery and Energy Reliability and North American Electric Reliability Corporation, the number of reported weather-related power outages has increased dramatically in the recent years [30]. According to [31], approximately 78% of the outages from 1992 to 2010 were caused by extreme weather events affecting around 178 million metered customers and costing the U.S. economy 18–33 billion dollars per year [32]. Thus, the staggering cost of power system outages due to natural disasters combined with the impacts on personal safety and security from loss of critical services calls for an urgent need to ensure resilience in complex electric power networks [33], [34]. Along this line, the U.S. DOE launched the Smart Grid Investment Grant program, funded by $3.4 billion invested through the American Recovery and Reinvestment Act of 2009 to modernize the nation's electricity system. Some of the benefits of investing in smart grid technologies, tools, and techniques include synchrophasor technologies, remote terminal units, distribution automation, including sensors and advanced meters for faster utility responses to power outages, and the ability to restore services more quickly compared to traditional outage management techniques, thus resulting in less inconvenience and lower outage cost for customers.

B. Control of DG-Energized Islands

A DG-supplied intentional island that is formed in the proposed restoration approach can be thought of as a small single-source microgrid employed to restore additional critical loads during an extreme event. In the case of a single-source microgrid, the single grid-forming resource operates in the isochronous mode and easily maintain a stable islanded operation. In the isochronous mode, the generator maintains a constant speed regardless of the load. The DG used for restoration can be clean or fossil-fuel-based generators as long as they can operate in the isochronous mode. Similarly, a diesel generator placed for emergency conditions can operate in the isochronous mode. Thus, during islanded operation, the local generation profile of the DG can be modified to reduce the imbalance between local load and generation and reduce the disconnection transient [35]. If there are no synchronous machines to balance demand and supply, the inverters should also be responsible for frequency control during islanded operation through its frequency control scheme [36]. Note that a PV+battery can be made to operate in the isochronous mode using grid-forming inverter technology [37]. However, only a PV (with no battery) will not be conducive for an isochronous mode operation and thus cannot be employed to energize islands. It is worth mentioning that the small customer-owned PVs modeled in this article are grid-following devices and do not actively contribute to maintaining voltage and frequency within the island. Note that restoration using multisource islanding is difficult, as it requires additional consideration to including mechanisms for power-sharing and voltage and frequency control for multiple DGs operating in the isochronous mode. Thus, we have proposed employing only single-source energized islands for restoration.

C. Performance Comparison

In the past, modern heuristic algorithms such as GA [6], [38], simulated annealing [39], and particle swarm optimization [7] have been used for various combinatorial optimization problems, including service restoration in power systems [40]. In this section, we compare the performance of the proposed approach against one of the soft computing algorithms, GA. Other popular algorithms for DSR in the existing literature include: 1) optimization approach that uses an MINLP model [9], [10]; and 2) a search-based approach using a spanning-tree algorithm [11], [12]. However, we select the GA for the performance comparison because 1) the MINLP based methods are not scalable for large systems; and 2) search-based methods (spanning tree) are not applicable as the number of possible operational topologies in the test case is in the order of millions.

The approach to simulate the GA for the restoration problem is detailed next. Once the genetic representation (switch status (0/1) in our case) is defined, the GA proceeds to initialize a population of solutions and then to improve it through repetitive application of the mutation, crossover, and selection operators. Following are the steps.

1) *Initialization:* We select the initial population by Monte Carlo simulation. To do this, 100 different random faults in the test case are simulated, and we use the previously described MILP formulation to get spanning trees, which are our initial population.
2) In the GA, offspring represents solutions that combine characteristics of their parents. To provide this heritability, a crossover operator must build a spanning tree that consists mostly of edges found in the parents. This is achieved by applying Kruskal random spanning tree [41] to the graph $\mathcal{G} = (\mathcal{V}, \mathcal{T}_1 \cup \mathcal{T}_2)$, where $\mathcal{V}$ is the set of vertices and $\mathcal{T}_1$ and $\mathcal{T}_2$ are the edge sets of the parental trees. A mutated chromosome usually represents a solution similar to that of its parent. To provide this locality, a mutation operator must make a small change in a parent's solution. This means that a mutated chromosome should represent a spanning tree that consists mostly of edges also found in its parent. This can be done by removing a random edge from $\mathcal{T}$ and replacing it with a new edge (normally open switch) that reconnects the tree.
3) Load not served (LNS) is calculated as the difference between total loads and our primary objective function as defined in (1) to evaluate the fitness

$$\text{LNS} = \sum_{i\in\mathcal{V}} \sum_{\phi\in\{a,b,c\}} P_{Li}^{\phi} - \sum_{i\in\mathcal{V}} \sum_{\phi\in\{a,b,c\}} s_i\, P_{Li}^{\phi}. \quad (15)$$

The average simulation time for MILP is around 12.3 s. We allowed free convergence with the GA for several random faults in the proposed test case. It was observed that the GA failed to give the converged solution for more than an hour as finding the optimal spanning tree takes a huge number of iterations. Thus, for a reasonable comparison, we set the maximum allowed computational time to be 3 min. Several random faults in the test case are simulated, and an average of those trials is taken for the performance comparison using three different measures: number of switching operations, simulation time, and percentage of load restored (in kilowatt) after a fault. It is observed that the best spanning tree given by the GA at the end of computation requires more number of switching operations. Additionally, with the given switching schemes, the percentage of total load restored is lower than the proposed approach. Thus, we claim that the quality of the solution from a GA for a given computational budget is poor than the proposed MILP formulation. The overall comparison is shown pictorially in Fig. 11.

It is worth mentioning that in addition to crossover and mutation, other heuristics may be employed to penalize the crossover between candidate solutions that are too similar; this encourages the diversity in the initial population and helps prevent premature convergence to a less optimal solution. However, improving the GA is not within the scope of this article.

D. Key Findings

This section summarizes the results highlighting the major achievements and key findings of the proposed approach. 1) We studied the impact of emerging smart grid technologies, including DGs and remote-controlled switches, to enhance the self-healing capability and allow faster recovery. Remote-controlled switches allow load transfer among the feeders, and DGs allow the active islanding scheme to restore the outage loads during faults in the system. Islands are sized dynamically based on the fault scenarios, available resources, and load priority. 2) The proposed approach is generic enough to simulate any kind of event in the distribution feeder. The formulation we discussed prioritizes the feeder restoration over the islanding scheme, thus reducing the requirement for islanded operation using the backup DGs unless required (see Table I). 3) An optimal operation of customer-owned DGs helps improve the restorability during an extreme event by reducing the customer load demand, thus allowing grid-forming DGs to restore additional loads. 4) The proposed approach is scalable and generates a feasible restoration plan quickly, thus making it applicable to a real-world distribution feeder for service restoration. Besides, any new additional resources can be incorporated into the formulation without any additional complexity.

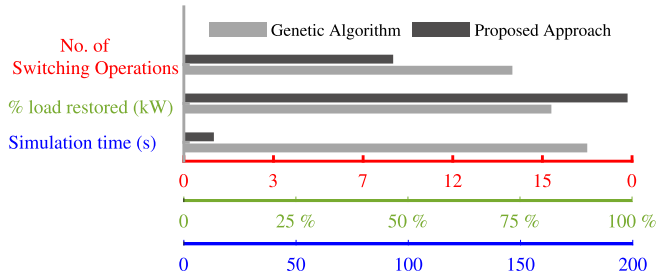

Fig. 11. Performance comparison with the GA. Three different measures are compared against the proposed approach, and color of the X-axis corresponds to each measure labeled in the Y-axis.

VI. Conclusion and Future Work

DSR, although widely studied in the existing literature, still requires attention due to the growing service reliability and resilience expectations from the increasingly complex power distribution systems. In this article, we proposed an optimal and scalable framework for the restoration of a large-scale three-phase unbalanced power distribution network that combines the normal feeder restoration with active islanding methods during extreme events into one unified framework. The proposed framework is generic, and the parameters and network models used in the formulation can be easily tweaked to represent a real-world system and a real-world fault/damage scenario. It is demonstrated that the restored network from either feeder reconfiguration or DG-assisted islands operates in a radial topology by selecting optimal and power flow feasible restoration paths. The formulation can handle multiple sources (feeders or DGs) without significantly increasing the computational complexity. Moreover, we also quantified the resilience value provided by grid-following/customer-owned DGs by evaluating the improvement in restoration capability.

The emerging smart grid technologies, such as remote-controlled switches and DG islanding, pose additional complexity to the service restoration problem especially under cold load pick up (CLPU) conditions. Thus, the sequence of operation for the complete restoration and recovery process needs to be studied to better execute these advanced algorithms with due

consideration to DG energization and CLPU events. Furthermore, this article can be enhanced by exploring the infrastructure recovery phase, where DG-assisted islands can be synchronized and eventually connected to the grid. An intentional island supplied by multiple grid-forming/grid-supporting DGs may also appear when trying to synchronize the multiple single-source islands as the infrastructure recovers. In such a case, a distributed/decentralized secondary controller that is collocated with the grid-forming DGs can be used for voltage and frequency restoration to enable the formation and operation of such multi-source dynamically formed islands.

REFERENCES

[1] National Academies of Sciences, Engineering, and Medicine, Enhancing the Resilience of the Nation's Electricity System. Washington, DC, USA: National Academies Press, 2017.

[2] M. Panteli and P. Mancarella, "The grid: Stronger bigger smarter?: Presenting a conceptual framework of power system resilience," *IEEE Power Energy Mag.*, vol. 13, no. 3, pp. 58–66, May/Jun. 2015.

[3] Y. Wang, C. Chen, J. Wang, and R. Baldick, "Research on resilience of power systems under natural disasters—A review," *IEEE Trans. Power Syst.*, vol. 31, no. 2, pp. 1604–1613, Mar. 2016.

[4] C.-C. Liu, S. J. Lee, and S. Venkata, "An expert system operational aid for restoration and loss reduction of distribution systems," *IEEE Trans. Power Syst.* , vol. 3, no. 2, pp. 619–626, May 1988.

[5] K. N. Miu, H.-D. Chiang, and R. J. McNulty, "Multi-tier service restoration through network reconfiguration and capacitor control for large-scale radial distribution networks," *IEEE Trans. Power Syst.*, vol. 15, no. 3, pp. 1001–1007, Aug. 2000.

[6] Y. Kumar, B. Das, and J. Sharma, "Service restoration in distribution system using non-dominated sorting genetic algorithm," *Electr. Power Syst. Res.*, vol. 76, nos. 9/10, pp. 768–777, 2006.

[7] Z. Li, X. Chen, K. Yu, Y. Sun, and H. Liu, "A hybrid particle swarm optimization approach for distribution network reconfiguration problem," in *Proc. IEEE PES GM-Convers. Del. Elect. Energy 21st Century*, 2008, pp. 1–7.

[8] J. Lei, Y. Deng, Y. He, and B. Zhang, "Network reconfiguration in unbalanced distribution systems for service restoration and loss reduction," in *Proc. IEEE Power Eng. Soc. Winter Meeting*, 2000, vol. 4, pp. 2345–2350.

[9] S. Khushalani, J. M. Solanki, and N. N. Schulz, "Optimized restoration of unbalanced distribution systems," *IEEE Trans. Power Syst.*, vol. 22, no. 2, pp. 624–630, May 2007.

[10] Z. Wang and J. Wang, "Self-healing resilient distribution systems based on sectionalization into microgrids," *IEEE Trans. Power Syst*, vol. 30, no. 6, pp. 3139–3149, Nov. 2015.

[11] J. Li, X.-Y. Ma, C.-C. Liu, and K. P. Schneider, "Distribution system restoration with microgrids using spanning tree search," *IEEE Trans. Power Syst.*, vol. 29, no. 6, pp. 3021–3029, Nov. 2014.

[12] H. Gao, Y. Chen, Y. Xu, and C.-C. Liu, "Resilience-oriented critical load restoration using microgrids in distribution systems," *IEEE Trans. Smart Grid*, vol. 7, no. 6, pp. 2837–2848, Nov. 2016.

[13] C. Chen, J. Wang, F. Qiu, and D. Zhao, "Resilient distribution system by microgrids formation after natural disasters," *IEEE Trans. Smart Grid*, vol. 7, no. 2, pp. 958–966, Mar. 2016.

[14] M. Ahmadi, M. E. Lotfy, A. M. Howlader, A. Yona, and T. Senjyu, "Centralised multi-objective integration of wind farm and battery energy storage system in real-distribution network considering environmental, technical and economic perspective," *IET Gener., Transmiss. Distrib.*, vol. 13, no. 22, pp. 5207–5217, 2019.

[15] B. Chen, C. Chen, J. Wang, and K. L. Butler-Purry, "Multi-time step service restoration for advanced distribution systems and microgrids," *IEEE Trans. Smart Grid*, vol. 9, no. 6, pp. 6793–6805, Nov. 2018.

[16] S. Poudel and A. Dubey, "Critical load restoration using distributed energy resources for resilient power distribution system," *IEEE Trans. Power Syst.*, vol. 34, no. 1, pp. 52–63, Jan. 2019.

[17] H. Zhai, M. Yang, B. Chen, and N. Kang, "Dynamic reconfiguration of three-phase unbalanced distribution networks," *Int. J. Elect. Power Energy Syst.*, vol. 99, pp. 1–10, 2018.

[18] B. Chen, C. Chen, J. Wang, and K. L. Butler-Purry, "Sequential service restoration for unbalanced distribution systems and microgrids," *IEEE Trans. Power Syst.*, vol. 33, no. 2, pp. 1507–1520, Mar. 2018.

[19] J. Kirk, *Count Loops in a Graph*, MathWorks, Natick, MA, USA. [Online]. Available: https://www.mathworks.com/matlabcentral/fileexchange/10722-count-loops-in-a-graph, Accessed: Jan. 9, 2019.

[20] L. Gan and S. H. Low, "Convex relaxations and linear approximation for optimal power flow in multiphase radial networks," in *Proc. IEEE Power Syst. Comput. Conf.*, 2014, pp. 1–9.

[21] W. L. Winston, M. Venkataramanan, and J. B. Goldberg, *Introduction to Mathematical Programming*, vol. 1. Pacific Grove, CA, USA: Thomson/Brooks/Cole Duxbury, 2003.

[22] H. Ahmadi and J. R. Martı, "Linear current flow equations with application to distribution systems reconfiguration," *IEEE Trans. Power Syst.*, vol. 30, no. 4, pp. 2073–2080, Jul. 2015.

[23] H. Marzooghi, D. J. Hill, and G. Verbic, "Aggregated demand modelling including distributed generation, storage and demand response," 2014, *arXiv:1412.3143*.

[24] M. Panteli, P. Mancarella, D. N. Trakas, E. Kyriakides, and N. D. Hatziargyriou, "Metrics and quantification of operational and infrastructure resilience in power systems," *IEEE Trans. Power Syst.*, vol. 32, no. 6, pp. 4732–4742, Nov. 2017.

[25] S. Poudel, A. Dubey, and A. Bose, "Risk-based probabilistic quantification of power distribution system operational resilience," *IEEE Syst. J.*, to be published, doi: 10.1109/JSYST.2019.2940939.

[26] K. P. Schneider, Y. Chen, D. Engle, and D. Chassin, "A taxonomy of north american radial distribution feeders," in *Proc. IEEE Power Energy Soc. Gen. Meeting*, 2009, pp. 1–6.

[27] M. Ahmadi, M. E. Lotfy, R. Shigenobu, A. M. Howlader, and T. Senjyu, "Optimal sizing of multiple renewable energy resources and pv inverter reactive power control encompassing environmental, technical, and economic issues," *IEEE Syst. J.*, vol. 13, no. 3, pp. 3026–3037, Sep. 2019.

[28] M. Ahmadi, M. E. Lotfy, R. Shigenobu, A. Yona, and T. Senjyu, "Optimal sizing and placement of rooftop solar photovoltaic at Kabul city real distribution network," *IET Gener., Transmiss. Distrib.*, vol. 12, no. 2, pp. 303–309, 2017.

[29] Smart Grid Investments Improve Grid Reliability, Resilience, and Storm Responses, Nov. 2014. [Online] Available: https://www.energy.gov/sites/prod/files/2014/12/f19/SG-ImprovesRestoration-Nov2014.pdf

[30] A. Kenward and U. Raja, "Blackout: Extreme weather climate change and power outages," *Climate Central*, vol. 10, pp. 1–23, 2014.

[31] R. J. Campbell, "Weather-related power outages and electric system resiliency," Congressional Res. Service, Library of Congress, Washington, DC, USA, Tech. Rep. R42696, 2012.

[32] A. M. Salman, Y. Li, and M. G. Stewart, "Evaluating system reliability and targeted hardening strategies of power distribution systems subjected to hurricanes," *Rel. Eng. Syst. Saf.*, vol. 144, pp. 319–333, 2015.

[33] CNN, *3 Storms, 3 Responses: Comparing Harvey, Irma and Maria*. [Online]. Available: https://www.cnn.com/2017/09/26/us/response-harvey-irma-maria/index.html, Accessed: Jan. 5, 2019.

[34] W. House, *Economic Benefits of Increasing Electric Grid Resilience to Weather Outages*," Washington, DC, USA: Executive Office of the President, 2013.

[35] J. P. Lopes, C. Moreira, and A. Madureira, "Defining control strategies for microgrids islanded operation," *IEEE Trans. Power Syst.*, vol. 21, no. 2, pp. 916–924, May 2006.

[36] F. Katiraei, M. R. Iravani, and P. W. Lehn, "Micro-grid autonomous operation during and subsequent to islanding process," *IEEE Trans. Power Del.*, vol. 20, no. 1, pp. 248–257, Jan. 2005.

[37] J.-Y. Kim *et al.*, "Cooperative control strategy of energy storage system and microsources for stabilizing the microgrid during islanded operation," *IEEE Trans. Power Electron.*, vol. 25, no. 12, pp. 3037–3048, Dec. 2010.

[38] I. Watanabe and I. Kurihara, "A genetic algorithm for optimizing switching sequence of service restoration," in *Proc. 15th Power Syst. Comput. Conf.*, Liege, 2005, p. 6.

[39] Y.-J. Jeon, J.-C. Kim, J.-O. Kim, J.-R. Shin, and K. Y. Lee, "An efficient simulated annealing algorithm for network reconfiguration in large-scale distribution systems," *IEEE Trans. Power Del.*, vol. 17, no. 4, pp. 1070–1078, Oct. 2002.

[40] S. Toune, H. Fudo, T. Genji, Y. Fukuyama, and Y. Nakanishi, "Comparative study of modern heuristic algorithms to service restoration in distribution systems," *IEEE Trans. Power Del.*, vol. 17, no. 1, pp. 173–181, Jan. 2002.

[41] G. R. Raidl and B. A. Julstrom, "Edge sets: An effective evolutionary coding of spanning trees," *IEEE Trans. Evol. Comput.*, vol. 7, no. 3, pp. 225–239, Jun. 2003.